Physics Letters B 718 (2012) 130–135

Contents lists available at SciVerse ScienceDirect

Physics Letters B

www.elsevier.com/locate/physletb

The quarkyonic phase and the Z_{N_c} symmetry

Yuji Sakai [a,*], Hiroaki Kouno [b], Takahiro Sasaki [c], Masanobu Yahiro [c]

[a] Quantum Hadron Physics Laboratory RIKEN Nishina Center, Saitama 351-0198, Japan
[b] Department of Physics, Saga University, Saga 840-8502, Japan
[c] Department of Physics, Graduate School of Sciences, Kyushu University, Fukuoka 812-8581, Japan

ARTICLE INFO

Article history:
Received 8 June 2012
Received in revised form 5 September 2012
Accepted 8 October 2012
Available online 11 October 2012
Editor: J.-P. Blaizot

ABSTRACT

We investigate the interplay between the $\mathbb{Z}_{N_c}$ symmetry and the emergence of the quarkyonic phase, adding the flavor-dependent complex chemical potentials $\mu_f = \mu + iT\theta_f$ with $(\theta_f) = (0, \theta, -\theta)$ to the Polyakov-loop extended Nambu–Jona-Lasinio (PNJL) model. When $\theta = 0$, the PNJL model with the μ_f agrees with the standard PNJL model with the real chemical potential μ. When $\theta = 2\pi/3$, meanwhile, the PNJL model with the μ_f has the $\mathbb{Z}_{N_c}$ symmetry exactly for any real μ, so that the quarkyonic phase exists at small T and large μ. Once θ varies from $2\pi/3$, the quarkyonic phase exists only on a line of $T = 0$ and μ larger than the dynamical quark mass, and the region at small T and large μ is dominated by the quarkyonic-like phase in which the Polyakov loop is small but finite.

Understanding of the confinement mechanism is one of the most important subjects in hadron physics. Lattice QCD (LQCD) shows numerically that QCD is in the confinement and chiral symmetry breaking phase at low temperature (T) and in the deconfinement and chiral symmetry restoration phase at high T. In the limit of infinite current quark mass, the Polyakov loop is an exact order parameter for the deconfinement transition, since the $\mathbb{Z}_{N_c}$ symmetry is exact there. The chiral condensate is, meanwhile, an exact order parameter for the chiral restoration in the limit of zero current quark mass. In the real world where u and d quarks have small current masses, the chiral condensate is considered to be a good order parameter for the chiral restoration, but there is no guarantee that the Polyakov loop is a good order parameter for the deconfinement transition.

In the previous paper [1], we have proposed a QCD-like theory with the $\mathbb{Z}_{N_c}$ symmetry. Let us start with the SU(N_c) gauge theory with N_f degenerate flavors to construct the QCD-like theory. The partition function Z of the SU(N_c) gauge theory is obtained in Euclidean space–time by

$$Z = \int DqD\bar{q}DA \exp[-S_0] \tag{1}$$

with the action

$$S_0 = \int d^4x \left[\sum_f \bar{q}_f (\gamma_\nu D_\nu + m_f) q_f + \frac{1}{4g^2} F_{\mu\nu}^2 \right], \tag{2}$$

where q_f is the quark field with flavor f and current quark mass m_f, $D_\nu = \partial_\nu - iA_\nu$ is the covariant derivative with the gauge field A_ν, g is the gauge coupling and $F_{\mu\nu} = \partial_\mu A_\nu - \partial_\nu A_\mu - i[A_\mu, A_\nu]$. The temporal boundary condition for quark is

$$q_f(x, \beta = 1/T) = -q_f(x, 0). \tag{3}$$

The fermion boundary condition is changed by the $\mathbb{Z}_{N_c}$ transformation as [2,3]

$$q_f(x, \beta) = -\exp(-i2\pi k/N_c) q_f(x, 0) \tag{4}$$

for integer k, while the action S_0 keeps the form of (2) in virtue of the fact that the $\mathbb{Z}_{N_c}$ symmetry is the center symmetry of the gauge symmetry [2]. The $\mathbb{Z}_{N_c}$ symmetry thus breaks down through the fermion boundary condition (3) in QCD.

Now we consider the SU(N) gauge theory with N degenerate flavors, i.e. $N = N_c = N_f$, and assume the twisted boundary condition (TBC) in the temporal direction [1]:

$$q_f(x, \beta) = -\exp(-i\theta_f) q_f(x, 0) \tag{5}$$

with the twisted angles

$$\theta_f = 2\pi(f-1)/N + \theta_1 \tag{6}$$

for flavors f labeled by integers from 1 to N, where θ_1 is an arbitrary real number in a range of $0 \leqslant \theta_1 < 2\pi$. The action S_0 with the TBC is a QCD-like theory proposed in Ref. [1]. In fact, the QCD-like theory has the $\mathbb{Z}_{N_c}$ symmetry, since f is changed into $f+k$ by the $\mathbb{Z}_N$ transformation but $f+k$ can be relabeled by f. In the QCD-like theory, the Polyakov loop becomes an exact order parameter of the deconfinement transition. The QCD-like theory then becomes a quite useful theory to understand the confinement mechanism.

* Corresponding author.
E-mail addresses: ysakai@riken.ac.jp (Y. Sakai), kounoh@cc.saga-u.ac.jp (H. Kouno), sasaki@phys.kyushu-u.ac.jp (T. Sasaki), yahiro@phys.kyushu-u.ac.jp (M. Yahiro).

0370-2693
http://dx.doi.org/10.1016/j.physletb.2012.10.027

When the fermion field q_f is transformed by

$$q_f \to \exp(-i\theta_f T\tau) q_f \tag{7}$$

with the twisted angle θ_f and the Euclidean time τ, the action S_0 is changed into

$$S(\theta_f) = \int d^4x \Bigg[\sum_f \bar{q}_f (\gamma_\nu D_\nu - i\theta_f T\gamma_4 + m_f) q_f + \frac{1}{4g^2} F_{\mu\nu}^2 \Bigg] \tag{8}$$

with the imaginary chemical potential $\mu_f = iT\theta_f$, while the TBC returns to the standard one (3). The action S_0 with the TBC is thus identical with the action $S(\theta_f)$ with the standard one (3). In the limit of $T = 0$, the action $S(\theta_f)$ comes back to the QCD action S_0 with the standard boundary condition (3) kept. The QCD-like theory thus agrees with QCD at $T = 0$ where the Polyakov loop Φ is zero. One can then expect that in the QCD-like theory Φ is zero up to some temperature T_c and becomes finite above T_c, i.e., that the $\mathbb{Z}_{N_c}$ symmetry is exactly preserved below T_c but spontaneously broken above T_c. Actually, this behavior is confirmed by imposing the TBC on the Polyakov-loop extended Nambu–Jona-Lasinio (PNJL) model [3–21]. The PNJL model with the TBC [1] is referred to as the TBC model in this Letter. In the TBC model, the flavor symmetry is explicitly broken by the flavor-dependent TBC (5), but the flavor-symmetry breaking is recovered at $T < T_c$. The TBC model is thus a model proper to understand the confinement mechanism.

A current topic related to the confinement is the quarkyonic phase [10,11,13,20,22]. It is a confined (color-singlet) phase with finite quark-number density n, that is, a phase with $\Phi = 0$ and $n \neq 0$. The n-generation induces the chiral restoration; in fact, the two phenomena occur almost simultaneously in the PNJL model [21]. This fact indicates that the quarkyonic phase can be regarded as a chirally-symmetric and confined phase. It was suggested in Refs. [23,24] that the chirally-broken phase is enlarged toward lager μ by the chiral density wave. In this Letter, for simplicity, we ignore inhomogeneous condensates such as the chiral density wave. Effects of the inhomogeneous condensate on the quarkyonic phase and the interplay between the effects and the $\mathbb{Z}_{N_c}$ symmetry are interesting as a future work. The concept of the quarkyonic phase was constructed in large N_c QCD. In fact, the phase was first found at small T and large real quark-number chemical potential μ in large N_c QCD. Recently, the PNJL model showed that a quarkyonic-like phase with $\Phi < 0.5$ and $n \neq 0$ exists at small T and large μ for the case of $N_c = 3$ [13,20]. This result may stem from the fact that the deconfinement transition is crossover for $N_c = 3$. This suggests that the quarkyonic phase can survive even at $N_c = 3$ in the QCD-like theory with the $\mathbb{Z}_{N_c}$ symmetry.

In this Letter, we consider the PNJL model of $N \equiv N_c = N_f = 3$ with the flavor-independent real chemical potential μ and the flavor-dependent quark boundary condition (5) with

$$(\theta_f) = (0, \theta, -\theta) \tag{9}$$

instead of (6); see Fig. 1 for the boundary condition. The present system is the same as that with the standard boundary condition (3) and the flavor-dependent complex chemical potentials $\mu_f = \mu + iT\theta_f$ with (9). The present model with the μ_f is reduced to the standard PNJL model with the flavor-independent real chemical potential μ when $\theta = 0$ and to the TBC model with the $\mathbb{Z}_{N_c}$ symmetry when $\theta = 2\pi/3$. Varying θ, one can see how the phase diagram is changed between the exact color-confinement in the TBC model and the approximate one in the standard PNJL model. The aim of this Letter is to see this behavior. Our particular interest is the location of the quarkyonic and the quarkyonic-like phase in the μ–T plane.

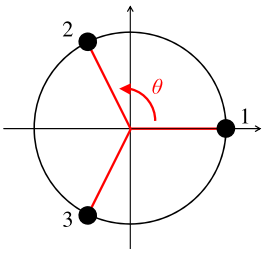

Fig. 1. Location of $\exp[i\theta_f]$ in the complex plane; here, $(\theta_f) = (0, \theta, -\theta)$.

In general, there is no guarantee that the QCD partition function with complex chemical potential is real. It is, however, possible to prove that the QCD partition function $Z_0(\mu_f)$ with $\mu_f = \mu + iT\theta_f$ is real. The fermion determinant $\det \mathcal{M}(\mu_f)$ satisfies the relation

$$\begin{aligned} \big[\det \mathcal{M}(\mu_f)\big]^* &= \det \mathcal{M}\big(-\mu_f^*\big) \\ &= \prod_f \det\big[D - (\mu - i\theta_f T)\gamma_4 + m_f\big] \\ &= \prod_f \det\big[D - (\mu + i\theta_f T)\gamma_4 + m_f\big] \\ &= \det \mathcal{M}(-\mu_f), \end{aligned} \tag{10}$$

where the third equality is obtained by the relabeling of the f. The present system thus has the sign problem, but the partition function is real, since

$$Z_0(\mu_f)^* = Z_0(-\mu_f) = Z_0(\mu_f), \tag{11}$$

where the first equality is obtained by (10) and the second one by the charge conjugation. Also in the PNJL model with the μ_f, the partition function is real, as shown later.

The three-flavor PNJL Lagrangian is defined in Euclidean space–time as

$$\begin{aligned} \mathcal{L} = \bar{q}(\gamma_\nu D_\nu + \hat{m} - \mu\gamma_4)q - G_S \sum_{a=0}^{8} \big[(\bar{q}\lambda_a q)^2 + (\bar{q} i\gamma_5 \lambda_a q)^2\big] \\ + G_D\Big[\det_{ij} \bar{q}_i(1+\gamma_5)q_j + \text{h.c.}\Big] + \mathcal{U}\big(\Phi[A], \Phi^*[A], T\big), \end{aligned} \tag{12}$$

where $D_\nu = \partial_\nu - i\delta_{\nu 4} A_4$, λ_a is the Gell-Mann matrices and $\hat{m} = \text{diag}(m_1, m_2, m_3)$. G_S and G_D are coupling constants of the scalar-type four-quark and the Kobayashi–Maskawa–'t Hooft (KMT) interaction [25,26], respectively. The KMT interaction breaks the $U_A(1)$ symmetry explicitly. The Polyakov loop Φ and its conjugate Φ^* are defined by

$$\Phi = \frac{1}{3}\text{tr}_c(L), \qquad \Phi^* = \frac{1}{3}\text{tr}_c(\bar{L}), \tag{13}$$

with $L = \exp(iA_4/T)$ in the Polyakov gauge. We take the Polyakov potential of Ref. [8]:

$$\begin{aligned} \mathcal{U} = T^4 \Bigg[-\frac{a(T)}{2}\Phi^*\Phi + b(T)\ln\big(1 - 6\Phi\Phi^* + 4\big(\Phi^3 + \Phi^{*3}\big) \\ - 3\big(\Phi\Phi^*\big)^2\big) \Bigg], \end{aligned} \tag{14}$$

$$a(T) = a_0 + a_1\left(\frac{T_0}{T}\right) + a_2\left(\frac{T_0}{T}\right)^2, \qquad b(T) = b_3\left(\frac{T_0}{T}\right)^3. \tag{15}$$

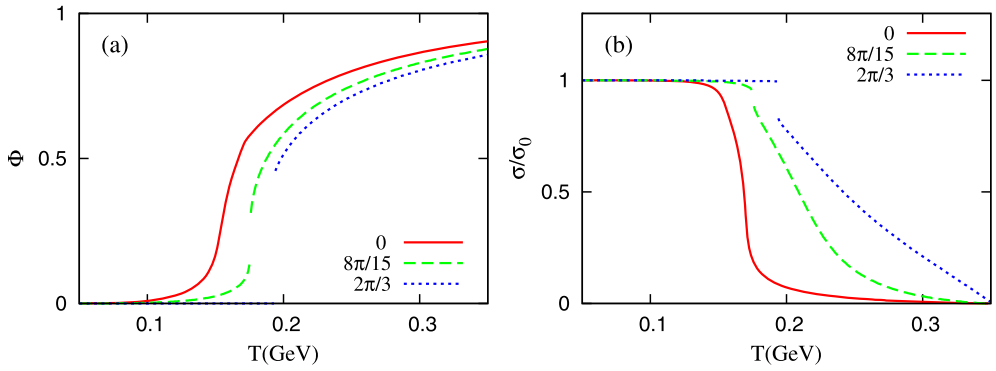

Fig. 2. (a) The Polyakov loop Φ and (b) the chiral condensate σ_1 in the θ–T plane at $\mu = 0$ MeV.

Table 1
Summary of the parameter set in the Polyakov-potential sector determined in Ref. [8]. All parameters are dimensionless.

a_0	a_1	a_2	b_3
3.51	−2.47	15.2	−1.75

Table 2
Summary of the parameter set in the NJL sector. All the parameters except m_0 are the same as in Ref. [32].

m_0 (MeV)	Λ (MeV)	$G_S\Lambda^2$	$G_D\Lambda^5$
5.5	602.3	1.835	12.36

Parameters of $\mathcal{U}$ are fitted to LQCD data at finite T in the pure gauge limit. The parameters except T_0 are summarized in Table 1. The Polyakov potential yields the first-order deconfinement phase transition at $T = T_0$ in the pure gauge theory [27,28]. The original value of T_0 is 270 MeV determined from the pure gauge LQCD data, but the PNJL model with this value yields a larger value of the pseudocritical temperature T_c at zero chemical potential than $T_c \approx 160$ MeV predicted by full LQCD [29–31]. We then rescale T_0 to 195 MeV so as to reproduce $T_c = 160$ MeV [19].

Now we consider the flavor-dependent complex chemical potential $\mu_f = \mu + i\theta_f T$. The thermodynamic potential (per volume) is obtained by the mean-field approximation as [16]

$$\Omega = \Omega_{\rm Q}(\sigma_f, \Phi, T, \mu_f) + U_{\rm M}(\sigma_f) + \mathcal{U}(\Phi, T) \tag{16}$$

with

$$\Omega_{\rm Q} = -2\sum_{f=1}^{3}\int \frac{d^3\mathbf{p}}{(2\pi)^3}\,{\rm tr}_c\Big[E_f + \frac{1}{\beta}\ln\big(1 + Le^{-\beta E_f^-}\big) + \frac{1}{\beta}\ln\big(1 + Le^{-\beta E_f^+}\big)\Big], \tag{17}$$

where $\sigma_f = \langle\bar{q}_f q_f\rangle$, $E_f^\pm = E_f \pm \mu_f$ and $E_f = \sqrt{\mathbf{p}^2 + M_f{}^2}$. Here the three-dimensional cutoff is taken for the momentum integration in the vacuum term [16]. Obviously, Ω is real. The dynamical quark masses M_f and the mesonic potential $U_{\rm M}$ are defined by

$$M_f = m_f - 4G_S\sigma_f + 2G_D|\epsilon_{fgh}|\sigma_g\sigma_h, \tag{18}$$

$$U_{\rm M} = \sum_f 2G_S\sigma_f^2 - 4G_D\sigma_1\sigma_2\sigma_3, \tag{19}$$

where ϵ_{fgh} is the antisymmetric symbol.

The PNJL model has six parameters (G_S, G_D, m_1, m_2, m_3, Λ). A typical set of the parameters is obtained in Ref. [32] for the $2+1$ flavor system with $m_1 = m_2 \equiv m_l < m_3$. The parameter set is fitted to empirical values of η'-meson mass and π-meson mass and π-meson decay constant at vacuum. In the present Letter, we set $m_0 \equiv m_l = m_3$ in the parameter set of Ref. [32]. The parameter set thus determined is shown in Table 2.

Taking the color summation in (16) leads to

$$\Omega = -2\sum_f\int\frac{d^3\mathbf{p}}{(2\pi)^3}\Big[3E_f + \frac{1}{\beta}(\ln\mathcal{F}_f + \ln\mathcal{F}_{\bar{f}})\Big] + U_{\rm M}(\sigma_f) + \mathcal{U}(\Phi, T), \tag{20}$$

where

$$\mathcal{F}_f = 1 + 3\Phi e^{-\beta E_f^-} + 3\Phi^* e^{-2\beta E_f^-} + e^{-3\beta E_f^-}, \tag{21}$$

$$\mathcal{F}_{\bar{f}} = 1 + 3\Phi^* e^{-\beta E_f^+} + 3\Phi e^{-2\beta E_f^+} + e^{-3\beta E_f^+}. \tag{22}$$

Note that $\mathcal{F}_2$ ($\mathcal{F}_{\bar{2}}$) is the complex conjugate to $\mathcal{F}_3$ ($\mathcal{F}_{\bar{3}}$), indicating that Ω is real.

In the case of $\theta = 2\pi/3$, particularly, Ω is invariant under the $\mathbb{Z}_3$ transformation,

$$\Phi \to e^{-i2\pi k/3}\Phi, \qquad \Phi^* \to e^{i2\pi k/3}\Phi^*. \tag{23}$$

Namely, Ω possesses the $\mathbb{Z}_3$ symmetry. When the exact color-confinement with $\Phi = 0$ occurs, Ω is invariant for any interchange among $E_1^\pm$, $E_2^\pm$ and $E_3^\pm$. Namely, Ω has the flavor symmetry in the exact color-confinement phase.

Fig. 2 shows T dependence of (a) the Polyakov loop Φ and (b) the chiral condensate σ_1 at $\mu = 0$. The solid, dashed and dotted curves represent three cases of $\theta = 0$, $8\pi/15$ and $2\pi/3$, respectively. For $\theta = 0$ corresponding to the standard boundary condition, the chiral and deconfinement transitions are both crossover. For $\theta = 2\pi/3$ corresponding to the TBC, the first-order deconfinement transition occurs at $T = T_c = 203$ MeV and the exact color-confinement phase appears below T_c. The first-order transition of Φ at $T = T_c$ propagates to σ_f as a discontinuity. For $\theta \neq 2\pi/3$, the deconfinement transition is no longer exact. As θ decreases from $2\pi/3$ to zero, T dependence of Φ becomes slower, and near $\theta = \pi/2$ the order of the deconfinement transition is changed from the first-order to crossover.

Fig. 3 shows the phase diagram in the T–μ plane. Panels (a)–(c) correspond to three cases of $\theta = 0$, $8\pi/15$ and $2\pi/3$, respectively. The thick (thin) solid curve represents the first-order deconfinement (chiral) phase transition line, while the thick (thin) dashed curve corresponds to the deconfinement (chiral) crossover line defined by the peak of $d\Phi/dT$ ($d\sigma_f/dT$). For $\theta = 0$, the chiral and deconfinement transitions are both crossover at smaller μ, but

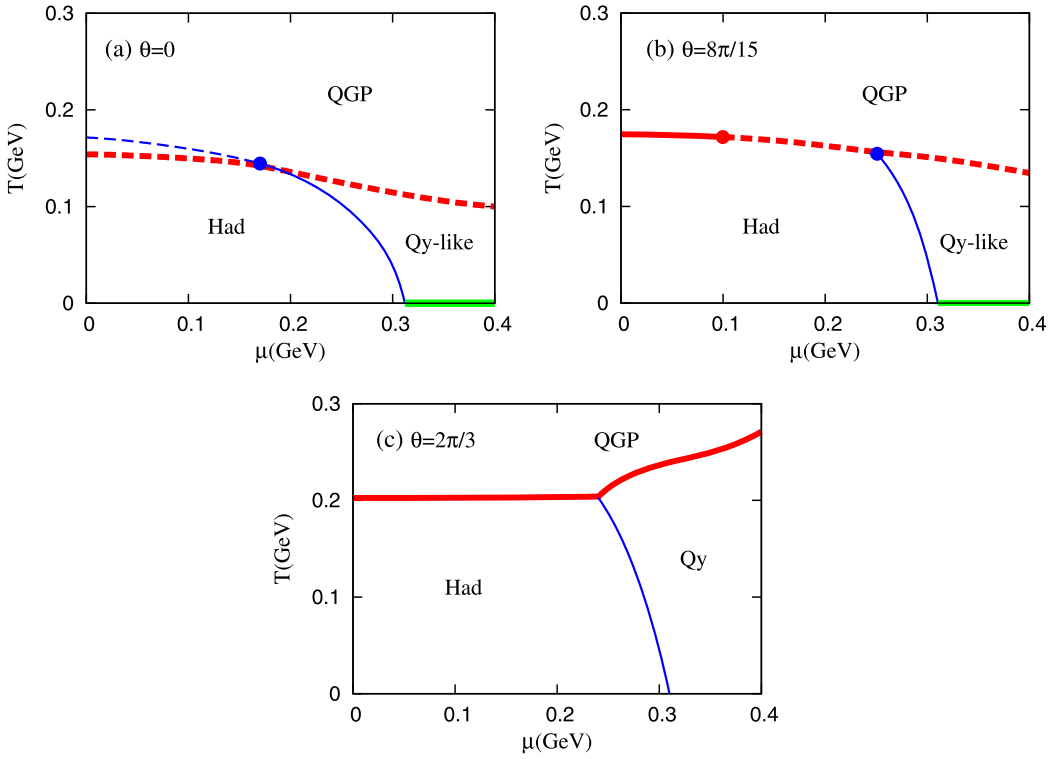

Fig. 3. Phase diagram in the T–μ plane. Panels (a)–(c) correspond to three cases of $\theta = 0$, $8\pi/15$ and $2\pi/3$, respectively. The thick (thin) solid curve means the first-order deconfinement (chiral) phase transition line, while the thick (thin) dashed curve does the deconfinement (chiral) crossover line. The closed circles stand for the endpoints of the first-order deconfinement and chiral phase transition lines. In panels (a) and (b), the thick solid line at $T = 0$ and $\mu \gtrsim M_f = 323$ MeV represents the quarkyonic phase.

the former becomes the first-order at larger μ. For $\theta = 2\pi/3$, the deconfinement transition is the first-order at any μ, whereas the first-order chiral transition line appears only at $\mu \approx M_f = 323$ MeV. The region labeled by "Qy" at $\mu \gtrsim M_f$ and small T is the quarkyonic phase, since $\Phi = 0$ and $n \neq 0$ there. The region labeled by "Had" is the hadron phase, because the chiral symmetry is broken there and thereby the equation of state is dominated by the pion gas [21]. The region labeled by "QGP" corresponds to the quark gluon plasma (QGP) phase, although the flavor symmetry is broken there by the TBC. As θ decreases from $2\pi/3$ to zero, the first-order chiral transition line declines toward smaller μ and the critical endpoint moves to smaller μ. Once θ varies from $2\pi/3$, the quarkyonic phase defined by $\Phi = 0$ and $n \neq 0$ shrinks on a line with $T = 0$ and $\mu \gtrsim M_f$ and a region at small T and $\mu \gtrsim M_f$ becomes a quarkyonic-like phase with small but finite Φ and $n \neq 0$; the latter region is labeled by "Qy-like".

For small θ far from $2\pi/3$, the deconfinement transition line declines as μ increases, but for $\theta = 2\pi/3$ the line is almost horizontal at small μ and rises at intermediate μ, as seen in Fig. 3. The rising of the deconfinement transition line is a consequence of the $\mathbb{Z}_3$ symmetry, as shown below. The quark one-loop part of Ω, which is defined by $\Omega_{\rm Q}$ in (17), can be expanded into a Maclaurin series

$$\Omega_{\rm Q} = \Omega_{\rm Q}\big(\Phi = 0, \Phi^* = 0\big) + c_{10}\Phi + c_{01}\Phi^* + c_{20}\Phi^2 + c_{11}\Phi\Phi^* + c_{02}\Phi^{*2} + \cdots. \tag{24}$$

The coefficients c_{nm} are explicitly obtained as

$$c_{10} = -\frac{18}{\beta}\sum_f \int \frac{d^3\mathbf{p}}{(2\pi)^3}\left(\frac{e^{-\beta E_f^-}}{1+e^{-3\beta E_f^-}} + \frac{e^{-2\beta E_f^+}}{1+e^{-3\beta E_f^+}}\right) < 0, \tag{25}$$

$$c_{01} = -\frac{18}{\beta}\sum_f \int \frac{d^3\mathbf{p}}{(2\pi)^3}\left(\frac{e^{-2\beta E_f^-}}{1+e^{-3\beta E_f^-}} + \frac{e^{-\beta E_f^+}}{1+e^{-3\beta E_f^+}}\right) < 0, \tag{26}$$

$$c_{20} = \frac{9}{\beta}\sum_f \int \frac{d^3\mathbf{p}}{(2\pi)^3}\left(\frac{e^{-2\beta E_f^-}}{(1+e^{-3\beta E_f^-})^2} + \frac{e^{-4\beta E_f^+}}{(1+e^{-3\beta E_f^+})^2}\right) > 0, \tag{27}$$

$$c_{11} = \frac{18}{\beta}\sum_f \int \frac{d^3\mathbf{p}}{(2\pi)^3}\left(\frac{e^{-3\beta E_f^-}}{(1+e^{-3\beta E_f^-})^2} + \frac{e^{-3\beta E_f^+}}{(1+e^{-3\beta E_f^+})^2}\right) > 0, \tag{28}$$

$$c_{02} = \frac{9}{\beta}\sum_f \int \frac{d^3\mathbf{p}}{(2\pi)^3}\left(\frac{e^{-4\beta E_f^-}}{(1+e^{-3\beta E_f^-})^2} + \frac{e^{-2\beta E_f^+}}{(1+e^{-3\beta E_f^+})^2}\right) > 0. \tag{29}$$

The c_{nm} are positive for even $n+m$ but negative for odd $n+m$. The absolute values of the c_{nm} increase as μ increases, unless μ is quite large. For simplicity, we fix M_f to a constant to focus our attention on Φ dependence of Ω. In this assumption, $U_{\rm M}$ and the zeroth-order term $\Omega_{\rm Q}(\Phi = 0, \Phi^* = 0)$ in the Maclaurin series are just constants and thereby become irrelevant to the present discussion. So we neglect these terms. We also assume that $\Phi = \Phi^*$. This is true for $\mu = 0$ and well satisfied for small and intermediate μ of our interest. In the pure gauge limit where $\Omega_{\rm Q} = 0$, the thermodynamic potential Ω agrees with the Polyakov potential $\mathcal{U}(\Phi)$ and hence has no μ dependence. The potential has a global minimum at $\Phi = 0$ and a local one at $\Phi = \Phi_m > 0$ for small T: namely, $\mathcal{U}(\Phi = 0) < \mathcal{U}(\Phi = \Phi_m)$. For the case of $\theta = 2\pi/3$, the system has

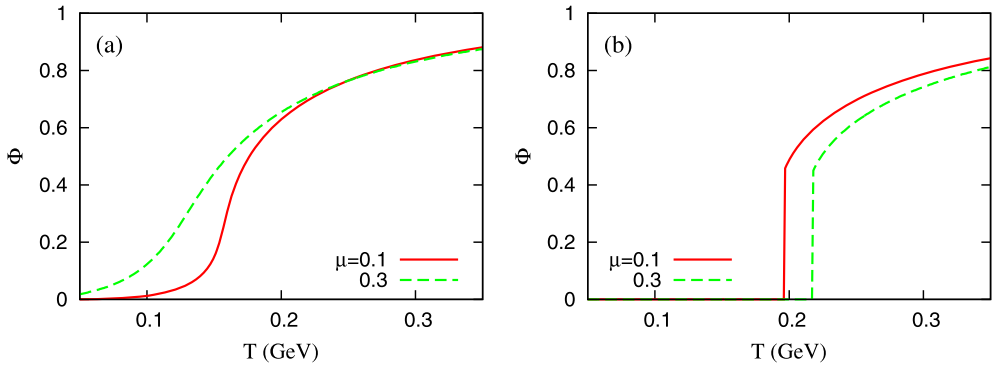

Fig. 4. T dependence of Φ for $\mu = 0.1, 0.3$ GeV in the lowest order approximation. Panel (a) corresponds to the case of $\theta = 0$ and panel (b) does to the case of $\theta = 2\pi/3$.

the $\mathbb{Z}_3$ symmetry. Up to the second-order of the Maclaurin series, only the $c_{11}\Phi\Phi^*$ term appears because of the symmetry. When the term is added to $\mathcal{U}$, the resultant potential keeps the same value as $\mathcal{U}(\Phi)$ at $\Phi = 0$, but increases from $\mathcal{U}(\Phi)$ at $\Phi > 0$. This property makes the deconfinement transition more difficult. The coefficient c_{11} as a function of μ little increases for $\mu \ll M_f$, but the increase becomes sizable for $\mu > M_f$. Therefore the rising of the deconfinement transition line with respect to increasing μ is tiny at small μ but becomes sizable at intermediate μ. The potential $c_{11}\Phi\Phi^* + \mathcal{U}$ keeps a positive curvature at $\Phi = 0$ because of $c_{11} > 0$, so that the deconfinement transition is first-order for any positive value of c_{11}. For the case of $\theta \neq 2\pi/3$, meanwhile, the first-order term $c_{10}\Phi + c_{01}\Phi^*$ is not prohibited by the $\mathbb{Z}_3$ symmetry and thereby dominates $\Omega_{\rm Q}$ particularly for small θ far from $2\pi/3$. Since c_{10} and c_{01} are negative, the situation for small θ becomes opposite to that for $\theta = 2\pi/3$. Eventually, the deconfinement transition line slopes down as μ increases for the case of small θ.

Fig. 4 shows T dependence of Φ for $\mu = 0.1, 0.3$ GeV. We consider the case of $\theta = 0$ in panel (a) and that of $\theta = 2\pi/3$ in panel (b) by assuming $\Omega = c_{10}\Phi + c_{01}\Phi^* + \mathcal{U}$ in panel (a) and $\Omega = c_{11}\Phi\Phi^* + \mathcal{U}$ in panel (b). Note that M_f is fixed to 323 MeV and T dependence of Φ is determined from the Ω with the minimum condition. As μ increases, the transition temperature decreases for $\theta = 0$, but increases for $\theta = 2\pi/3$. The transition is first-order for the case of $\theta = 2\pi/3$. These results are consistent with the qualitative discussion mentioned above.

In summary, we have investigated the interplay between the $\mathbb{Z}_{N_c}$ symmetry and the emergence of the quarkyonic phase, adding the complex chemical potentials $\mu_f = \mu + iT\theta_f$ with $(\theta_f) = (0, \theta, -\theta)$ to the PNJL model. When $\theta = 0$, the PNJL model with the μ_f is reduced to the PNJL model with real μ. This situation corresponds to QCD at real μ. When $\theta = 2\pi/3$, meanwhile, the PNJL model with the μ_f is reduced to the TBC model with the $\mathbb{Z}_{N_c}$ symmetry. This situation corresponds to the QCD-like theory with the $\mathbb{Z}_{N_c}$ symmetry at real μ. When $\theta = 2\pi/3$, the quarkyonic phase defined by $\Phi = 0$ and $n > 0$ really exists at small T and large μ. Once θ varies from $2\pi/3$ to zero, the $\mathbb{Z}_{N_c}$ symmetry is broken. As a consequence of this property, the quarkyonic phase exists only on a line of $T = 0$ and $\mu \gtrsim M_f$, and the region at small T and large μ is dominated by the quarkyonic-like phase characterized by small but finite Φ and $n > 0$. The $\mathbb{Z}_{N_c}$ symmetry thus plays an essential role on the emergence and the location of the quarkyonic phase in the μ–T plane, and the quarkyonic-like phase at $\theta = 0$ is a remnant of the quarkyonic phase at $\theta = 2\pi/3$. Since the $\mathbb{Z}_{N_c}$ symmetry is explicitly broken at $\theta = 0$, it is then natural to expand the concept of the quarkyonic phase and redefine it by a phase with small Φ and finite n. For this reason, the quarkyonic-like phase is often called the quarkyonic phase. The gross structure of the phase diagram thus has no qualitative difference between $\theta = 2\pi/3$ and zero, if the concept of the quarkyonic phase is properly expanded. In this sense, the $\mathbb{Z}_{N_c}$ symmetry is a good approximate concept for the case of $\theta = 0$, even if the current quark mass is small.

Acknowledgements

The authors thank A. Nakamura, T. Saito, K. Nagata and K. Kashiwa for useful discussions. H.K. also thanks M. Imachi, H. Yoneyama, H. Aoki and M. Tachibana for useful discussions. Y.S. is supported by RIKEN Special Postdoctoral Researchers Program. T.S. is supported by JSPS.

References

[1] H. Kouno, Y. Sakai, T. Makiyama, K. Tokunaga, T. Sasaki, M. Yahiro, J. Phys. G: Nucl. Part. Phys. 39 (2012) 085010.
[2] A. Roberge, N. Weiss, Nucl. Phys. B 275 (1986) 734.
[3] Y. Sakai, K. Kashiwa, H. Kouno, M. Yahiro, Phys. Rev. D 77 (2008) 051901(R).
[4] P.N. Meisinger, M.C. Ogilvie, Phys. Lett. B 379 (1996) 163.
[5] A. Dumitru, R.D. Pisarski, Phys. Rev. D 66 (2002) 096003;
A. Dumitru, Y. Hatta, J. Lenaghan, K. Orginos, R.D. Pisarski, Phys. Rev. D 70 (2004) 034511;
A. Dumitru, R.D. Pisarski, D. Zschiesche, Phys. Rev. D 72 (2005) 065008.
[6] K. Fukushima, Phys. Lett. B 591 (2004) 277.
[7] C. Ratti, M.A. Thaler, W. Weise, Phys. Rev. D 73 (2006) 014019;
C. Ratti, S. Rößner, M.A. Thaler, W. Weise, Eur. Phys. J. C 49 (2007) 213.
[8] S. Rößner, C. Ratti, W. Weise, Phys. Rev. D 75 (2007) 034007.
[9] B.-J. Schaefer, J.M. Pawlowski, J. Wambach, Phys. Rev. D 76 (2007) 074023.
[10] H. Abuki, R. Anglani, R. Gatto, G. Nardulli, M. Ruggieri, Phys. Rev. D 78 (2008) 034034.
[11] K. Fukushima, Phys. Rev. D 77 (2008) 114028.
[12] K. Kashiwa, H. Kouno, M. Matsuzaki, M. Yahiro, Phys. Lett. B 662 (2008) 26.
[13] L. McLerran, K. Redlich, C. Sasaki, Nucl. Phys. A 824 (2009) 86.
[14] T. Hell, S. Rößner, M. Cristoforetti, W. Weise, Phys. Rev. D 81 (2010) 074034;
T. Hell, K. Kashiwa, W. Weise, Phys. Rev. D 83 (2011) 114008.
[15] Y. Sakai, H. Kouno, M. Yahiro, J. Phys. G: Nucl. Part. Phys. 37 (2010) 105007.
[16] T. Matsumoto, K. Kashiwa, H. Kouno, K. Oda, M. Yahiro, Phys. Lett. B 694 (2011) 367.
[17] Y. Sakai, T. Sasaki, H. Kouno, M. Yahiro, Phys. Rev. D 82 (2010) 076003.
[18] R. Gatto, M. Ruggieri, Phys. Rev. D 83 (2011) 034016.
[19] T. Sasaki, Y. Sakai, H. Kouno, M. Yahiro, Phys. Rev. D 84 (2011) 091901.
[20] F. Buisseret, G. Lacroix, Phys. Rev. D 85 (2012) 016009.
[21] Y. Sakai, T. Sasaki, H. Kouno, M. Yahiro, J. Phys. G: Nucl. Part. Phys. 39 (2012) 035004.
[22] L. McLerran, R.D. Pisarski, Nucl. Phys. A 796 (2007) 83;
Y. Hidaka, L. McLerran, R.D. Pisarski, Nucl. Phys. A 808 (2008) 117.
[23] E. Nakano, T. Tatsumi, Phys. Rev. D 71 (2005) 114006.
[24] D. Nickel, Phys. Rev. Lett. 103 (2009) 072301;
D. Nickel, Phys. Rev. D 80 (2009) 074025;
S. Carignano, D. Nickel, M. Buballa, Phys. Rev. D 82 (2010) 054009.
[25] M. Kobayashi, T. Maskawa, Prog. Theor. Phys. 44 (1970) 1422;
M. Kobayashi, H. Kondo, T. Maskawa, Prog. Theor. Phys. 45 (1971) 1955.

[26] G. 't Hooft, Phys. Rev. Lett. 37 (1976) 8;
G. 't Hooft, Phys. Rev. D 14 (1976) 3432;
G. 't Hooft, Phys. Rev. D 18 (1978) 2199(E).
[27] G. Boyd, J. Engels, F. Karsch, E. Laermann, C. Legeland, M. Lütgemeier, B. Petersson, Nucl. Phys. B 469 (1996) 419.
[28] O. Kaczmarek, F. Karsch, P. Petreczky, F. Zantow, Phys. Lett. B 543 (2002) 41.
[29] S. Borsányi, Z. Fodor, C. Hoelbling, S.D. Katz, S. Krieg, C. Ratti, K.K. Szabo, arXiv: 1005.3508 [hep-lat], 2010.
[30] W. Söldner, arXiv:1012.4484 [hep-lat], 2010.
[31] K. Kanaya, arXiv:1012.4235 [hep-ph], 2010;
K. Kanaya, arXiv:1012.4247 [hep-ph], 2010.
[32] P. Rehberg, S.P. Klevansky, J. Hüfner, Phys. Rev. C 53 (1996) 410.